_____

An Intelligent Controller for the Signal Generation of Solar Energy and Battery Storage Supported Multi-Level UPQC

G. Mohan Babu [1], Dr. G. Suresh Babu [2], Dr. E. Vidya Sagar [3]

[1] Research scholar, Department of Electrical Engineering, Osmania University, Hyderabad, Telangana, India.

Email: mohanbabuguguloth1985@gmail.com

[2] Professor, Department of Electrical and Electronics Engineering, Chaitanya Bharathi Institute of Technology, Telangana, India.

Email: gsureshbabu_eee@cbit.ac.in

[3] Professor, Department of Electrical Engineering, Osmania University, Hyderabad, Telangana, India.

Email: evsuceou@gmail.com

Corresponding Author: Guguloth MohanBabu, Osmania University, Tel: +91 8328180776 mohanbabuguguloth1985@gmail.com

Abstract

This study examines, the solar power and battery energy storage associated diode clamped five-level unified Power quality conditioner (5L-UPQC) to handle the PQ related problems. To eliminate the requirement of the complex transformations like abc, dq0, αβ , the ANN based control scheme with LMBP training method is adopted for the 5L-UPQC to produce the necessary reference signals for the voltage source converters (VSC's). The prime goal of the proposed scheme is to maintain stable DLCV during load shifting, reduction of THD. In addition, the grid voltage distortions like sag, disturbance and swell were eliminated. The suggested method was demonstrated on two cases with several permutations of loads. However, to reveal the performance of the developed method, the comparison is carried out with the PIC and SMC.

Keywords: Unified Power Quality Conditioner, Power Quality, DC Link voltage balancing, and Artificial neural network

*Nomenclature***:**

UPQC	Unified Power Quality Conditioner
Five-level-UPQC	5L-UPQC
PV	Photovoltaic
BES	Battery Energy
PQ	Power Quality
SRF	SynchronousReference
p-q	InstantaneousReactive
ANN	Artificial Neural Network
PWM	Pulsewidth Modulation
LMBP	Levenberg- Marquardt Back Propagation
DLCV	DC Voltage across capacitor
THD	Total Harmonic Distortion
PF	PowerFactor
PIC	ProportionalIntegral Controller
SMC	Sliding Mode Control
FLC	Fuzzy Logic Controller
VSC	Voltage Source Converter
BC	Boost Converter
SHAPF	Shunt Active Power Filter

2932

_____

BBC	Buck Boost Converter
MSE	Meansquare Error
SEAF	Series Active Power Filter
ACO	Ant Colony Algorithm
FOPID	Fractional Order Proportional Integral Derivate
MSF	Membership Function
ANFIS	Artificial Neuro Fuzzy Interface System
V_{LL}	Line To Line RMS Voltage
CE	Change In Error
OL	Output Layer of ANN
IL	Input Layer of ANN
HL	Hidden Layer of ANN
E	Error
m	Modulation Index
$V_{cr,pp}$	Peak To Peak Voltage Ripple
Δi_{lmax}	Peak Ripple Current
V_m	Peak Voltage Of The System
a_f	Over Loading Factor
$f_{sh}\ f_{se}$	Switching Frequency
L_{se}	SEAF Inductance
V_{S_abc}	Source Voltage For ABC Phases
$R_S,\ L_S$	Grid Resistance and Inductance
V_{l_abc}	Phase voltage across load
C_{dc}	DC Link Capacitance
V_{se_abc}	Compensated phase voltage
$V^{ref}_{se\_abc}$	Reference Series Injected phase Voltage
V_{dc}	DC Link Voltage
i_{S_abc}	Source phase Current
i_{l_abc}	Load phase Current
R_{sh}	SHAPF Resistance
V^{ref}_{dc}	Reference DLCV
i_{sh_abc}	SHAPF Injected Current In Abc Phases
$i^{ref}_{sh\_abc}$	Reference SHAPF Injected Current In Abc Phases
i^{ref}_{dc}	Reference DC Current
R_{se}	SEAF Resistance
$V_{dc,err}$	DLCV Error
i^{ref}_{BS}	Reference current of the battery
L_{sh}	SHAPF Inductance
Δi_{dc}	DC error output
i_{ph}	Photocurrent Source

2933

_____

i_d	Forward Diode Current
$R_{s,PV}$, $R_{sh,PV}$ & i_{PV}, $i_{sh,PV}$	Series & Parallel Cell Resistances And Their Currents
K_i	Short-Circuited Current of the ith Cell
$i_{BS,err}$	Error current of the battery
i_{SC}	Short Circuit Current
q	Charge of an Electron
α	Diode Ideality Factor
k	Boltzmann's Constant
$i_{BS,er}^{*}$	Reference error current of the battery
T	Temperature of the Cell
G	Solar Irradiation
V_{oc}	Open-Circuit Voltage
N_s and N_p	PV Cells Connected in Series and Parallel
T_n	Nominal Temperature
E_g	Band Gap of Semi Conductor
$V_{b\_charge,b\_discharge}$	Battery Charge and Discharge Voltage
R	Internal Battery Resistance
i_b	Battery Current
E_0	Constant Voltage
Q	Battery Capacity
K	Polarization Constant

1. Introduction

Next, the PSO in association with the grey wolf based optimization algorithm was chosen to obtain the suitable FOPIDC controller parameters of SHAPF for compensating the reactive power while minimizing THD for the balance and unbalanced loads as the case studies with an experimental investigation [1]. However, to reduce the complexity the ANN was considered for UPQC reference signal generation to solve PQ issues [2]. An intelligent fuzzy-tuned PIC was developed for hybrid shunt active and passive filters with the specific aim of efficiently reducing current THD. To assess its performance, an analysis was conducted across different load conditions, employing Clarke's transformation [3].

Further, to regulate and to handle DLCV feed forward ANN has been suggested for PV in combination with wind was associated to UPQC [4]. A Biogeography based optimization (BBO) algorithm was selected to obtain optimal gain values of PIC and for fast action in fault identification with higher accuracy with a motive of stabilizing DLCV fluctuations [5]. The Improved bat and Moth Flame metaheuristic optimization methods were hybridized to solve the PQ issues by optimal selecting the gain values of PIC [6]. The fuzzy logic controller (FLC) was developed for SEAF of distribution network to minimize the current and voltage related PQ problems [7]. Besides, to address PQ problems

effectively the Soccer match optimization was chosen for the ANN controller (ANNC) bias and weights selection for the PV/battery linked UPQC [8]. Ant colony optimization (ACA) was chosen for selecting of gain parameters of PI controller for the SHAPF in order to reduce THD under several conditions of loading [9].

The ANN based method was suggested for 5L-UPQC to minimize THD and suppress voltage distortions [10]. The metaherustic firefly nature inspired algorithm was used to train ANNC was developed for the shunt VSC for the PV/battery UPQC with an aim of reducing the MSE thereby minimizing THD [11]. A hybrid control approach, combining the features of FLC and ANN, was suggested for the UPQC. This approach aimed to mitigate imperfections and distortions in grid voltage and source current while maintaining dynamic load balance in the DLCV [12]. The LMBP trained ANN controller was adopted for UPQC to solve the grid voltage and current problems successfully [13]. A Soccer-league optimization technique was put forward to optimize the selection of gain parameters for the PIC in the UPQC. This method was designed to effectively address both voltage fluctuations and current distortions [14].

Many literature article have primarily concentrated on different controllers using traditional control methods for UPQC, often involving difficult Park and Clarke's

2934

_____

transformations. In contrast, this manuscript introduces an ANN based approach for generating reference signals in a PV/battery-connected DC link UPQC. The prime contribution is as follows:

- LMBP trained ANN scheme is proposed to solar PV and battery systems are coupled to the DC link of 5L-UPQC to produce the effective reference signals to avoid the requirement of traditional abc-dq0-αβ0 conversions.

- The prime aim of developed scheme is to diminish the source current THD, and eliminating of grid voltage side troubles like (disturbance, swell, sag etc)

In addition, the designed method is examined on two test cases for different loading conditions to show it's superior performance with respect to the minimization of current waveform THD, and voltage waveform fluctuations. The performance was tested by comparing it with PIC and SMC techniques. Table 1 gives the literature review.

This article is organized in the following manner: Section2 presents the modeling of 5L-UPVBES, Section3 provides the proposed ANN controller, Section4 showcases the results and discussion, and, lastly, Section5 provides the concluding remarks for the manuscript.

Table 1: Literature

Ref [No]	Control		PQ Issues				Loads	
	Reference signal generation method	Control Technique	THD	DC Link stabilization	Sag/ swell	Disturbances	Non-linear sensitive load	Un-balanced load
[1]	p-q theory	FOPID	✓				✓	✓
[2]	ANN	ANN	✓	✓	✓	✓	✓	✓
[3]	SRF	FUZZY-PI	✓	✓			✓	
[4]	ANN	ANN	✓		✓		✓	✓
[5]	SRF	PI-BBO	✓		✓		✓	✓
[6]	SRF	ANFIS	✓				✓	✓
[7]	p-q	FUZZY	✓		✓		✓	
[8]	SRF	PPFFA	✓				✓	✓
[9]	SRF	PI-ACO	✓				✓	✓
[10]	ANN	ANN	✓	✓	✓		✓	✓
[11]	SRF	FF-ANN	✓	✓	✓	✓	✓	✓
Proposed 5L-UPVBES	ANNC	ANNC	✓	✓	✓	✓	✓	✓

2. Modelling of developed 5L-UPVBES

Figure 1 illustrates the suggested configuration of the 5L-UPVBES, where the PV system and batteries are linked to the DC link of the UPQC. The UPQC serves as a unified device, integrating both series and shunt filters. The SAPF aims to tackle voltage challenges on the grid side by supplying the necessary V_{se} via the injection transformer. Likewise, the SHAPF injects appropriate i_{sh} to diminish THD and ensure the stability of the dc voltage.

_____
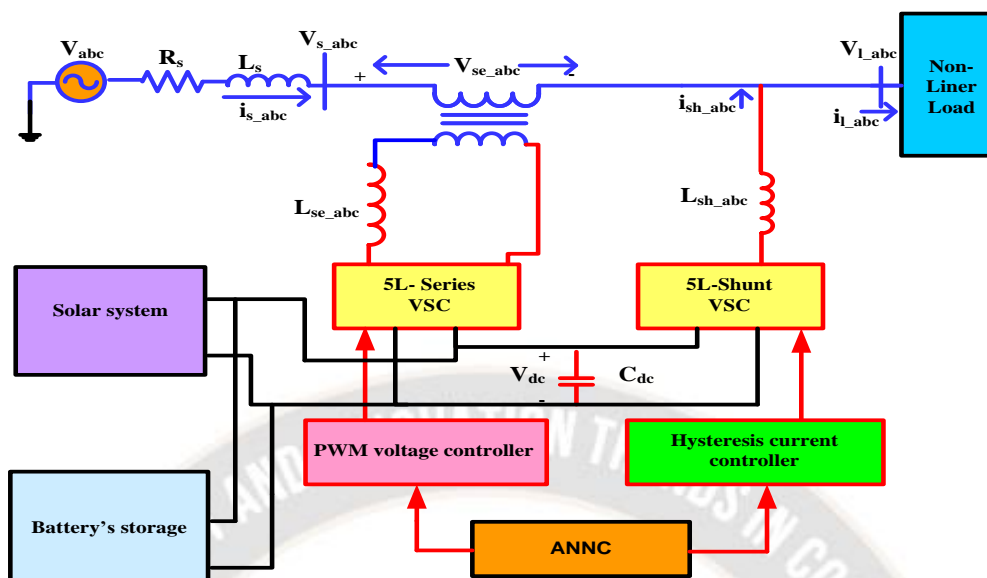
Figure 1: Proposed 5L-UPVBES configuration

Table 2: Switches ON/OFF for 5L diode clamped UPQC

V_{AN}	S1	S2	S3	S4	S'1	S'2	S'3	S'4
$V_{dc}/2$	✓	✓	✓	✓	*	*	*	*
$V_{dc}/4$	*	✓	✓	✓	✓	*	*	*
0	*	*	✓	✓	✓	✓	*	*
$-V_{dc}/4$	*	*	*	✓	✓	✓	✓	*
$-V_{dc}/2$	*	*	*	*	✓	✓	✓	✓

*Note: ✓ indictes ON , * indicates OFF
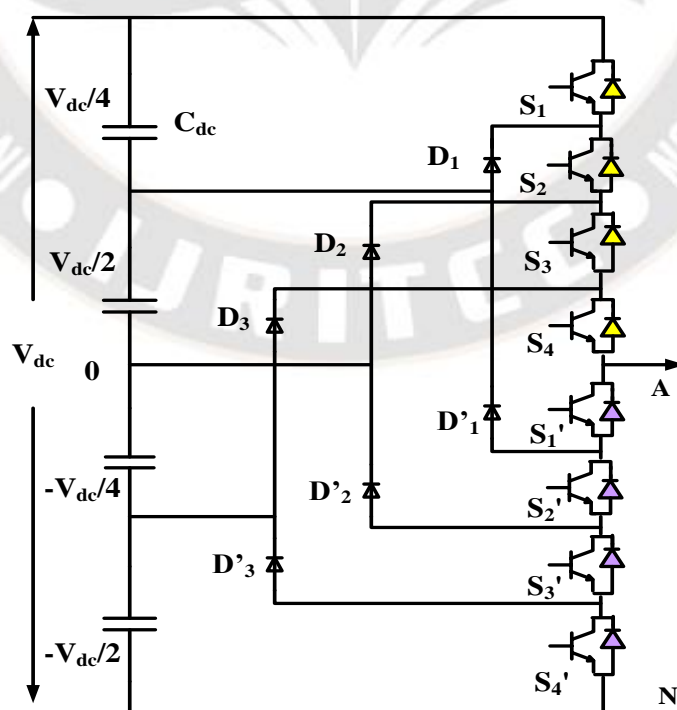
Figure 2: 5L Diode clamped single phase

_____

The most common multilevel arrangment is the diodeclamped inverter, whose output voltage is modulated by clamping the dc bus voltage using a diode clamping. Using diodes to reduce the voltage stress on the electrical equipment is the fundamental concept underlying this inverter. The voltage across each capacitor and switch is known as V_{dc}. A n-level converter requires (n-1)*(n-2) diodes, (n-1) voltage sources, and (2n-1) switching components. However, with the increase in the levels the distortions in the output is reduced thus becomes sinusoidal .A 5L diode clamped for single phase is shown in Figure 2. Table 2 lists the 5L diode clamped switching order.

2.1 Selection of C_{dc} and V_{dc}

From [29] under faulty condition, assume the shunt and series VSC's power handling capacity are 0.5XkVA and 2XkVA respectively. The kVA rating of VSC and V_{dc} are inversly proportional. By the change of 25% of V_{dc}, the equalent change in the energy across C_{dc} is calculated by Eq. (1)

$$\Delta E_{dc} = 1/2C_{dc}[(1.125V_{dc})^2 - (0.875V_{dc})^2] \tag{1}$$

Assume that for the suppose the load changes from 2XkVA to 0.5XkVA in 'n' cycles in 'T' sec, then the corresponding change in the system's energy is given by

$$\Delta E_s = (2X - X/2)n.T \tag{2}$$

By, equating Eq. (1) and (2), the C_{dc} is given by Eq. (3)

$$C_{dc} = \frac{2(2X - X/2)n.T}{(1.125V_{dc})^2 - (0.875V_{dc})^2} \tag{3}$$

Let, V_m is the peak voltage of the system and V_{dc} is m times to V_m. Where, 'm' modulation index varies between 1.2 and 2. However, %THD depends on L_{sh} and V_{dc} so the value of m is selected as 1.6 [29] for minimum THD. Therefore, V_{dc} is given by Eq. (4)

$$V_{dc} = 1.6*V_m \tag{4}$$

The V_{dc} for n level converter is evaluated by using [29] Eq. (5)

$$V^{ref}_{dc} = V_{dc}/(n-1) \tag{5}$$

2.2 Selection of coupling inductors for Shunt and series VSC

The coupling inductors which are adopted to connect the series and shunt VSC's to the source and the load are limited by di/dt and magnitude of currents. The ripple current peak value (Δi_{lmax}) take place at m=0.5, given in Eq. (6) is controlled by PWM [29].

$$\Delta i_{l\max} = V_{dc}/6f_{sw}L_{se} \tag{6}$$

Assuming the ripple current is about 10% of maximum peak to peak current given by Eq. (7)

$$\Delta i_{l\max} = 0.1*i_{\max} \tag{7}$$

Therefore, the maximum current handling by series capacitor in terms of power and phase voltage is given by Eq. (8). By using Eq. (6) and (8) L_{se} can be calculated.

$$i_{\max} = \frac{\sqrt{2}*P_r}{3*V_{ph}} \tag{8}$$

By heustrically testing [29] it has been identified that for m=1.6, V^{ref}_{dc}= 700, and L_{sh}= 15 mH the % THD is lower. The value of L_{sh} is given by Eq. (9)

$$i_{\max} = \frac{V_{dc}}{4.h.f_{sw\max}} \tag{9}$$

Where, h is the hysteresis band 5-10% .

2.3 Modeling of External support for 5L-UPQC DC Link

The solar/battery fed DC link is proposed for the diode clamped 5L-UPQC. It consists of a hybrid energy system solar and battery system to regulate the DLCV during the variation in loads. By providing the external support, the converter ratings and stress can be reduced with lowering the demands from the utility. The equation for DC link power demand (P_{dc}) of the suggested technique is given in equation (10).

$$P_{PV} + P_{BSS} - P_{dc} = 0 \tag{10}$$

2.3.1 PV system

In this research, the photovoltaic model is obtained from the Matlab/Simulink library its equivalent circuit is in Figure 3.
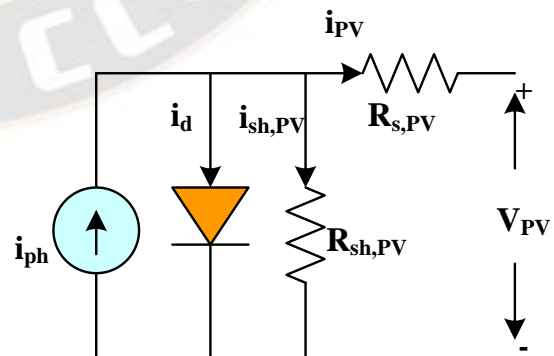
Figure 3: PV cell model

The PV cell effectively detects solar irradiation and transforms it into current. The i_{ph} for the PV module is

2937

_____

calculated using Eq. (11), while the reverse saturation current i_{rs} for the PV module is determined according to Eq. (12).

$$i_{ph} = [i_{SC} + K_i(T - 298)] * G / 1000 \qquad (11)$$

$$i_{rs} = i_{SC} / [\exp(qV_{oc} / N_s \eta kT) - 1] \qquad (12)$$

The module saturation current depends on cell temperature which is given by Eq. (13) and output current of module is given by Eq. (14)

$$i_{mo} = i_{rs}[T / T_n]^3 \exp[q * E_g / \eta k(1/T - 1/T_n)] \qquad (13)$$

$$i_{PV} = N_p * i_{ph} - N_p * i_{mo} * [\exp(V_{pv} / N_s + i_{PV} * (R_{s,PV}) / \qquad (14)$$

Where,

$$V_t = k * T / q$$

$$i_{sh,PV} = V_{PV} * ((N_p / N_s) + i_{PV} * R_{s,PV}) / R_{sh,PV} \qquad (15)$$

The output power is obtained by equation (16). The Figure 4 illustrates the solar cell characteristics under conditions of constant temperature and varying irradiation for 10 parallel and 18 series cells with rated power of 214.92W.

$$P_{PV} = V_{PV} \times i_{PV} \qquad (16)$$
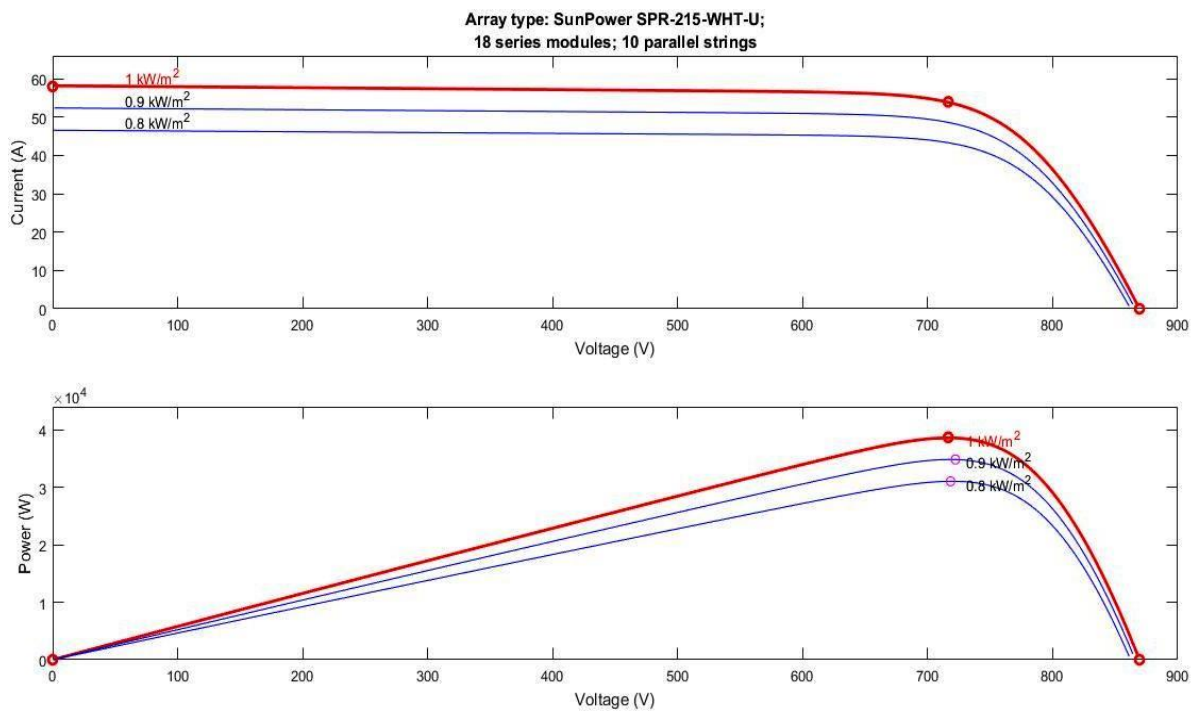
Figure 4: Solar characteristics under constant temperature of 25^0c with variable irrdaiation

2.3.2 Battery Energy storage (BES)

The BES system offers assistance in regulating DLCV. The cells in the battery are connected in parallel or series depending on the requirement of the voltage. In this work Li-ion battery is selected from simulink library because of its few benefits like low cost for maintenance and slower in discharge. The charge as well as discharge of the Li-ion type system is in Eq. (17)

$$V_b = V_{b\_charge,b\_discharge}(i_t, i*, i_b) - i_b R \qquad (17)$$

The charge and discharge of Li-ion type battery is given by Eq. (18).

$$E_{b\_charge} = E_0 - K(\frac{Q}{0.1Q + i_t})i* - K(\frac{Q}{Q - \int i_t dt})i_t + Ae^{-}$$

$$E_{b\_discharge} = E_0 - K(\frac{Q}{Q + i_t})i* - K(\frac{Q}{Q - \int i_t dt})i_t + Ae^{-b}$$

$$(18)$$

The *SOCOB* is calculated by Eq (19).

$$SOCOB = 50(1 + \int i_{BSS} \, dtQ) \qquad (19)$$

The PV will determine whether to charge or discharge the battery while adhering to the constraints specified in Eq. 20. The discharge of battery is shown in Fig. 5 for a nominal voltage of 650V with a rated capacity of 25Ah. The rating

2938

_____

selected for solar and battery systems are listed in Table 3. The control system of external power fed sources is given in Fig. 6.

$$SOCOB_{\min} \leq SOCOB \leq SOCOB_{\max} \tag{20}$$
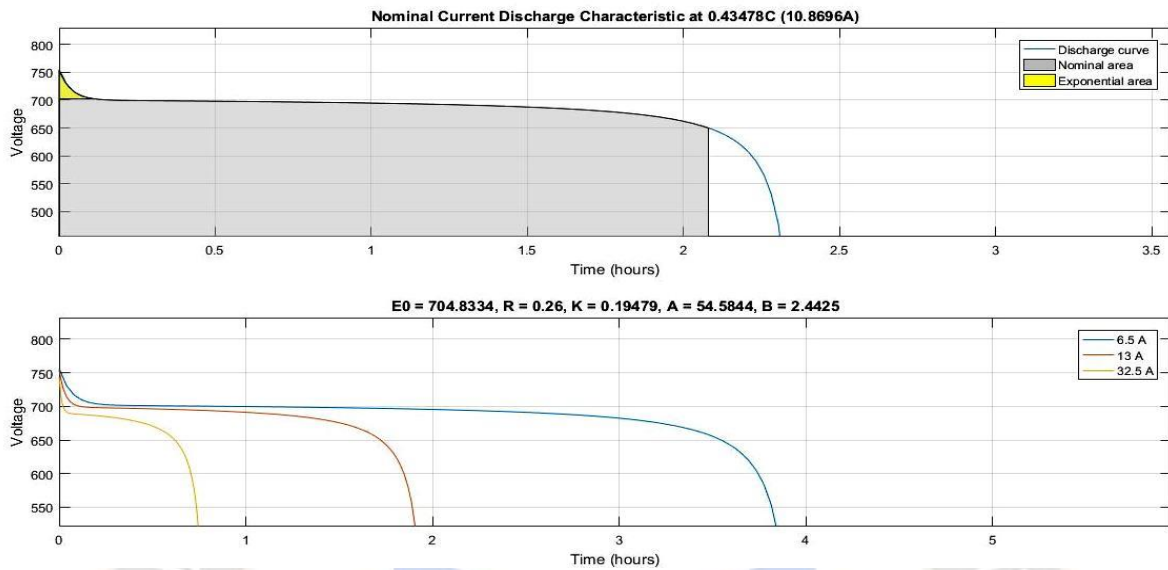
Figure 5: Characteristics of battery

3 ANN BASED PROPOSED SYSTEM

Changes generally occur at the distribution during frequent load variation. Moverover, within a short span of period, the system should be restored to its previous value in order to function normally. In this instance, the PWM method generates firing signal for the series VSC using the proposed ANNC.

3.1 SHAPF

The key task of shunt filter is to inject compensatory current to control DLCV under faults as well as dynamic loading circumstances and to suppress flaws in the current waveforms. An input, output and hidden layers make up the ANN structure. The IL passes the data it receives as input to the HL. When linked between the IL and HL, it is next multiplied by the appropriate weights on the connected links. Here, calculations are performed with a chosen bias on HL, and the outcomes are gathered in OL.
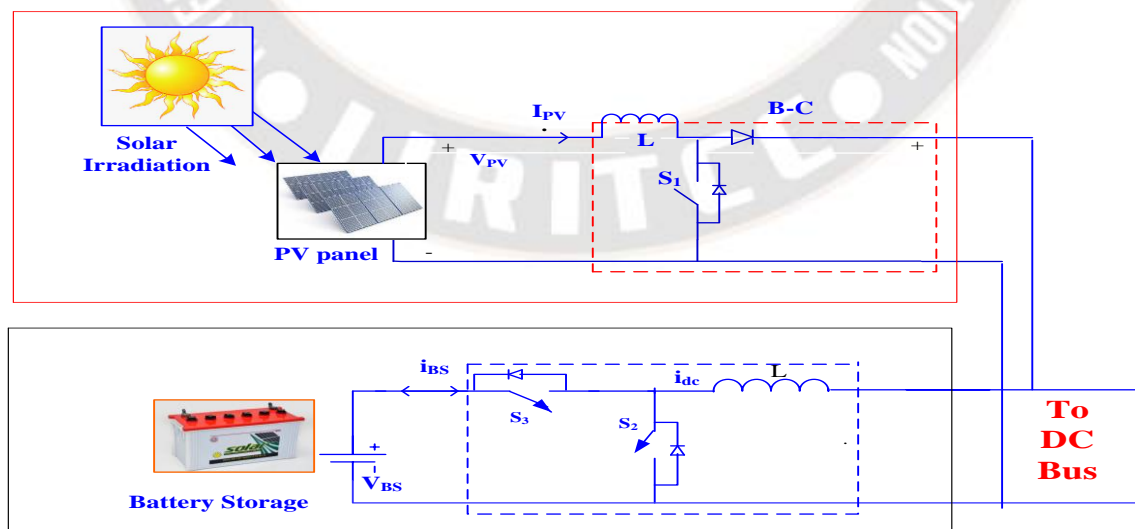
Figure 6: Control system for external supply sources

_____

Here, the LMBP trained ANN controller is chosen. To get the desired output, the weights of the link are adjusted during training by analyzing the mistake. For training the performance function is MSE is selected. The LMBP algorithm updates the weight using the generated derivatives, which have the advantages of rapid convergence and effective learning [32]. The ANN controller built for this DLCV balancing includes a single HL with 100 neurons and one input and output, as illustrated in Fig. 7.
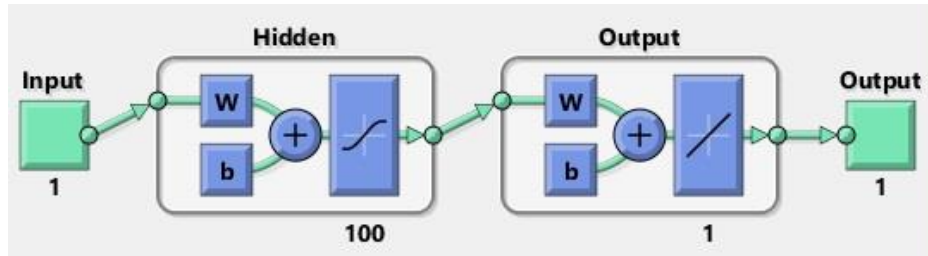
Figure 7: Structure of ANNC for DClink balancing
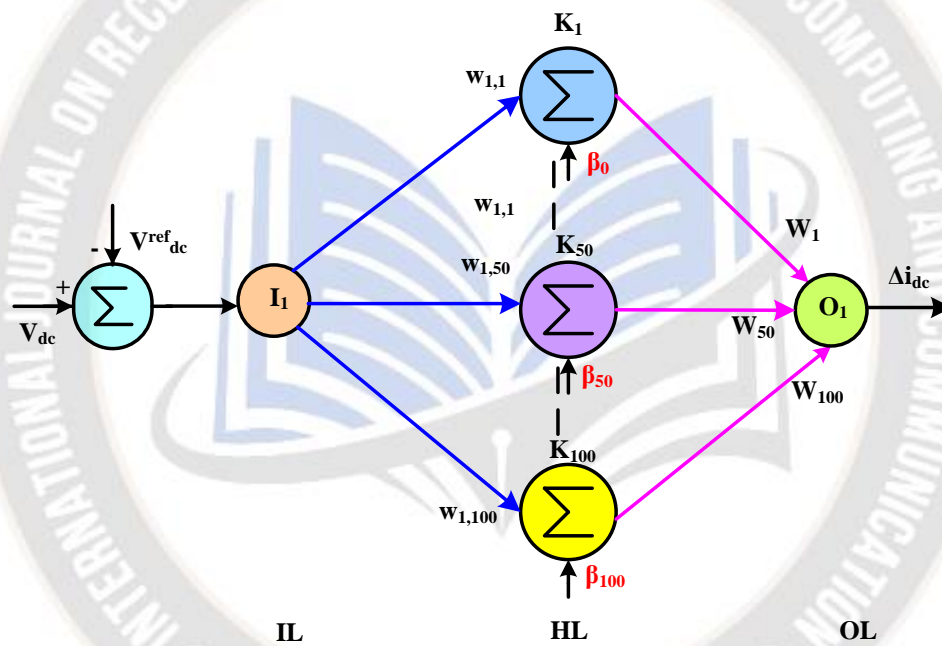
Figure 8: MLP for ANNC for DC link balancing

In multilayer perceptron networks, each neuron poses of a summation and activation functions. However, these neurons among the layers are interconnected with some numerical weights. The role of summation function is to add the bias with the multiplication of inputs with weights as given in Eq. (21). Where, β_k is a bias, w_{pk} is the weight joining p to k neuron, and m is inputs. In general, for nonlinearity the sigmoid function is considered as activation function shown by Eq. (22). Hence, the k neuron output is exhibited [24] in Eq. (23).

$$S_k = \sum_{p=1}^{m} w_{pk} I_p + \beta_k \quad (21)$$

$$f(x) = \frac{1}{1 + e^{-x}} \quad (22)$$

$$O_k = f_k \left(\sum_{p=1}^{m} w_{pk} I_p + \beta_k \right) \quad (23)$$

Mean square error is calculated by Eq. (24). However, O is the obtained output and $\overline{O}$ is expected, and n is the total number of instances.

$$MSE = \frac{1}{n} \sum_{p=1}^{m} (O_p - \overline{O}_p)^2 \quad (24)$$

The ANN is trained to produce reference current signals and to keep the DLCV constant. To keep the DLCV stable,

_____

V^{ref}_{dc} and V_{dc} are compared; the difference in error is selected as input, and i_{dc} is the target for ANN, as illustrated in figure 8. As illustrated in figure 9, the reference currents

signals ($i^{ref}_{sh\_abc}$) are regarded the target data while the load currents (i_{l_abc}) and DC error component (Δi_{dc}) are considered the input.
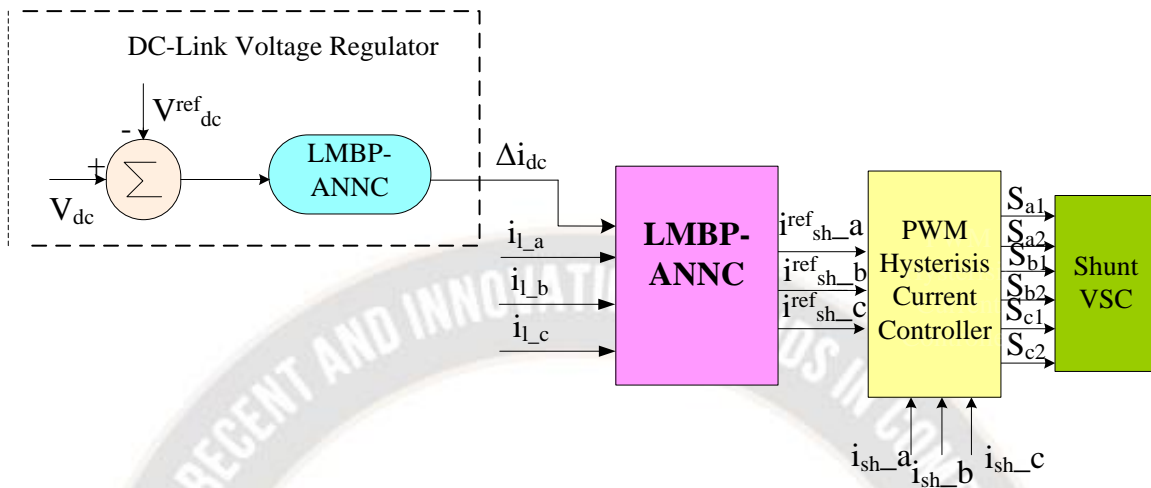
Figure 9: Shunt VSC Controller
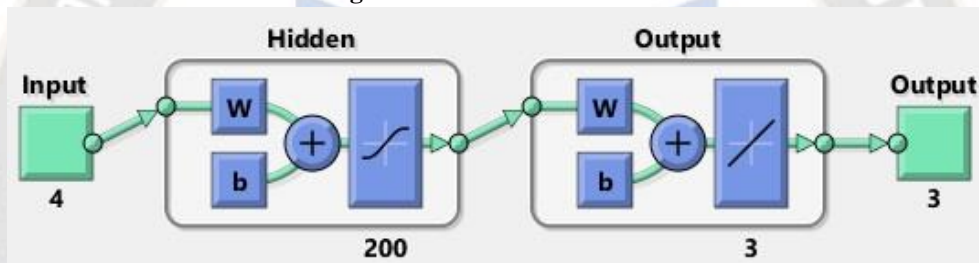
Figure 10: ANNC for SEAPF

3.2 Series VSC

The prominent role of SAPF is to suppress the voltage at grid distortions by injecting the proper V_{se} in order to maintain load voltage constant. The suggested series VSC reference signal generating strategy is exhibited in Fig 11,

and the arrangement of an ANN with an HIL of 200 neurons is illustrated in Figure 12. To generate the $V^{ref}_{se\_abc}$ the supply voltages ($V_{s\_abc,}$) are treated as input, whereas reference selected voltage as target to ANN.
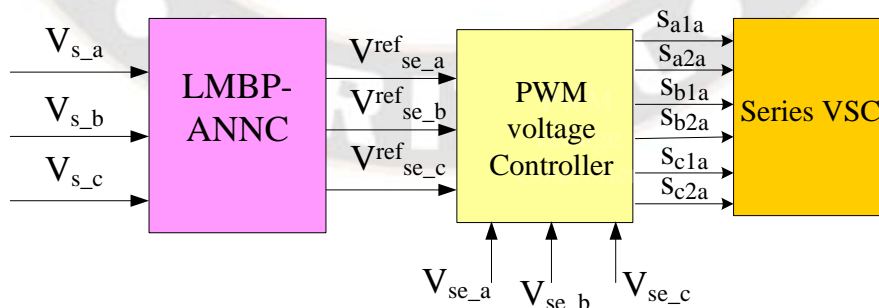
Figure 11: Series-VSC controller

_____
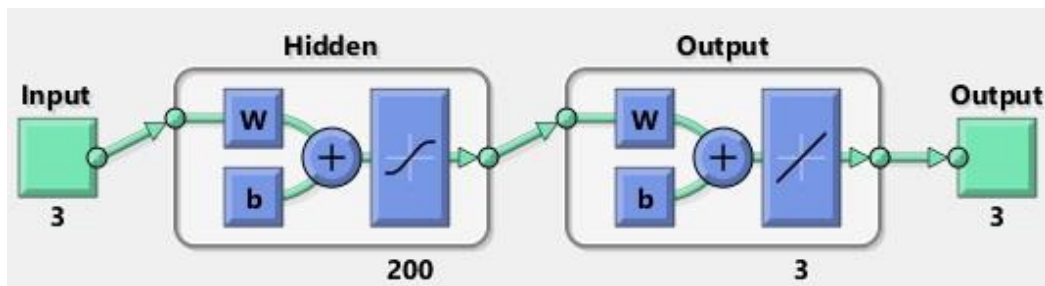
Figure 12: ANNC based reference signal generation for series VSC.

4 Results and Discussion

The recommended 5L-UPVBES in association of ANNC was created in Matlab. Figure 13 depicts the simulation model of the proposed model. The 5Level diode clamped model for UPQC is illustrated in Figure (13) with the proposed ANNC control strategy used for converters of UPQC. Table 3 displays the chosen system and the UPQC device settings. Here, two test studies with various permutations of voltage issues like sag, disturbance, swell, balanced and unbalanced loads with constant G and temperature of 25^0c were selected to revel the working of developed ANNC on 5L-UPVBES is given in Table 4. Both case-1 and case-2 take into account voltage sag, voltage swell, and voltage disturbance problems. However, in this work the reduction of current THD is considered as objective which is obtained by developed ANN for reference signal generation, and optimal selection of shunt and series controller parameters for diode clamped 5L-UPQC. To reveal the performance of the projected ANN, a comparison is

carried out with PIC and SMC methods at DLCV balancing. The THD is evaluated by Eq. (25).

$$THD = \frac{\sqrt{(I^2_2 + I^2_3 + ...I^2_n)}}{I_1} \qquad (25)$$

Where,

I_n= individual harmonic current distortion values in amps
I_1= individual harmonic current distortion values in amps
I_2= 2nd harmonic current distortion values in amps

The voltage sag/ swell ($V_{sag/swell}$) is evaluated by Eq. (26)

$$V_{sag/swell} = \frac{V_l - V_S}{V_l} = \frac{V_{se}}{V_l} \qquad (26)$$

The injected voltage by series filter is calculated by Eq. (27)

$$V_{se} = V_l - V_S \qquad (27)$$

The injected shunt filter current is calculated by Eq. (28)

$$i_{sh} = i_i - i_S \qquad (28)$$
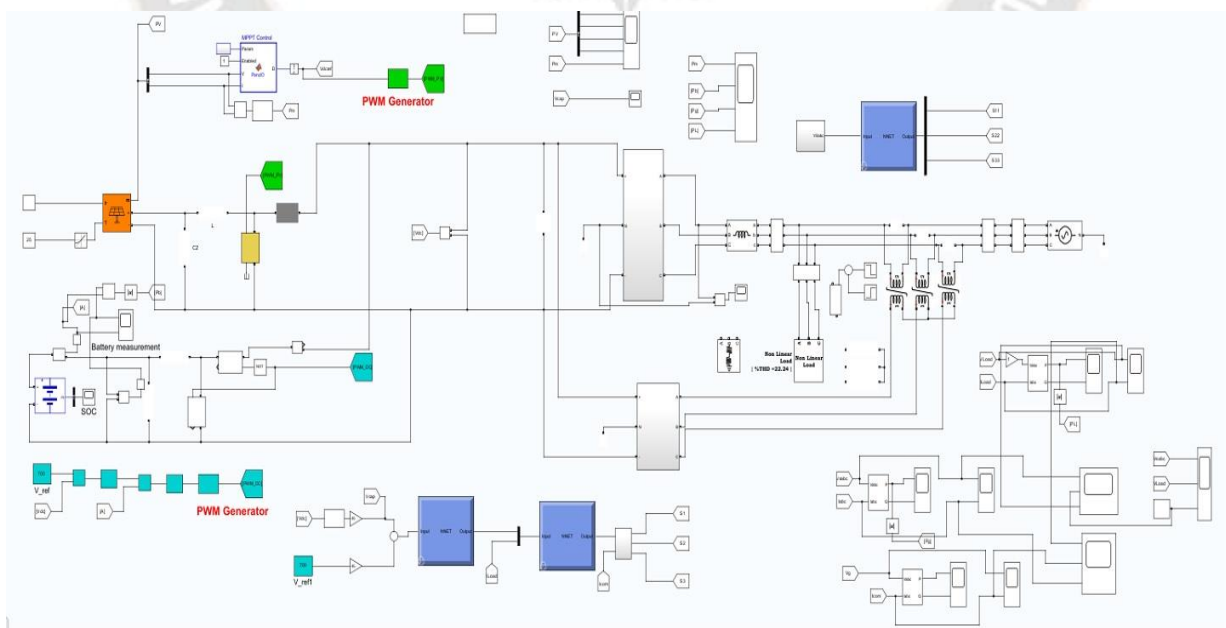
(a) Simulink model of total system
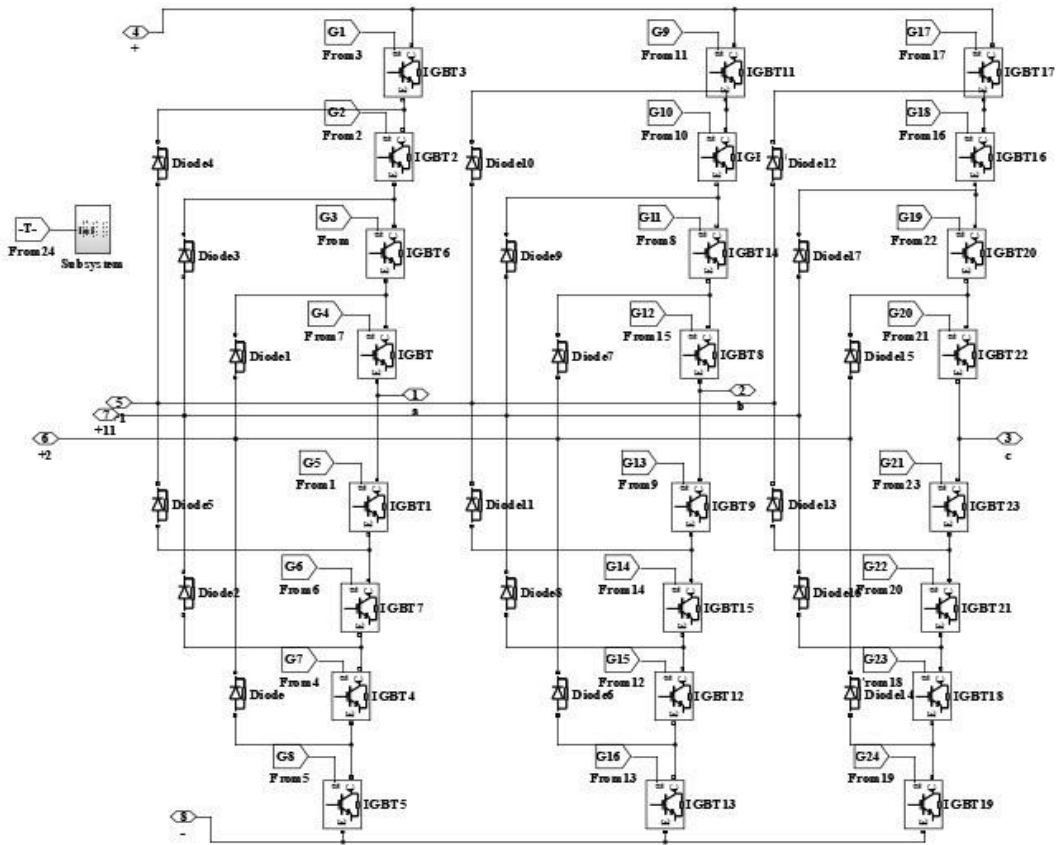
(a) Diode clamped 5-level VSC
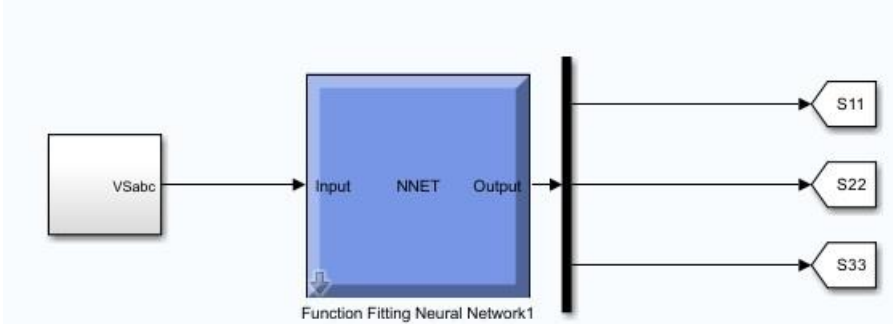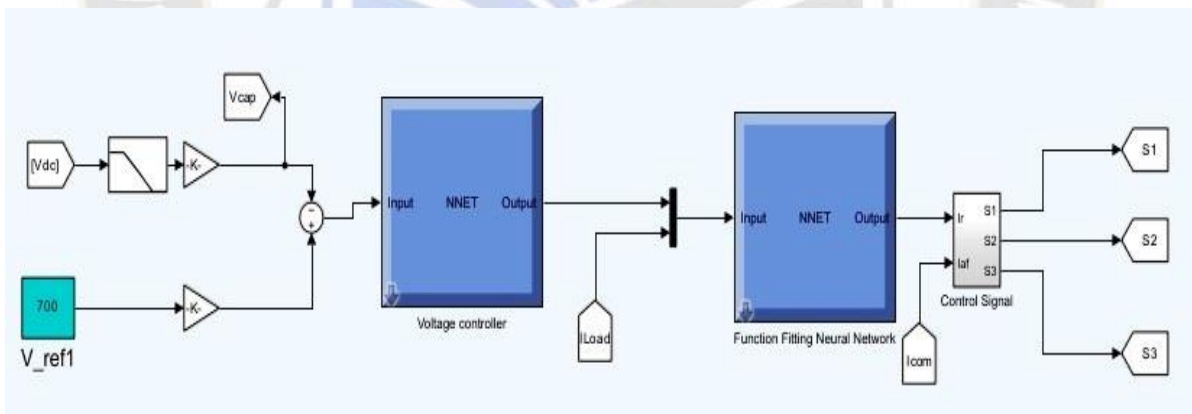
(b) Proposed ANN based reference signal generation controller scheme
Figure 13: Simulink model of the proposed system

_____

Table 3: System parameters

Grid Supply	R_s : 0.1ohm ; V_s : 415Volts ; L_s : 0.15 mH; f : 50Hertz
DLCV & inductors	C_{dc} : 2200μF; L_{se}= 6 mH, L_{sh}=15 mH
Loads	1. Balanced 3 Φ nonlinear load: P_L=3kW, Q_L=0.5 kVAR 2. Un-balanced load: P_{La}=3kW, Q_{La}=9 kVAR; P_{Lb}=4kW, Q_{Lb}=10 kVAR; P_{Lc}=4kW, Q_{Lc}=10 kVAR

Table 4: Test Cases studies considered for different loads

Condition	Case1	Case2
Source voltage V_{Sag} , V_{Swell} , disturbance	✓	✓
Current	✓	✓
Constant Irradiation 1000W/m2 and 25^0c temperature	✓	✓
THD (both V and I)	✓	✓
Load1	✓	
Load 2	✓	✓

During case 1, the supply voltage is disturbed for periods of 0.2 to 0.3, 0.4 to 0.5, and 0.6 to 0.7 seconds, respectively, as shown in Fig. 14(a). This case also exhibits 30% sag/swell. The suggested ANN approach effectively detects voltage sags, swells, and disturbances; it then supplies an appropriate correcting voltage via the interface transformer for keeping the load voltage stable. Besides, to exhibit the behavior of shunt filter with ANNC, Load 1 and 2 were chosen. From the Fig. 14(b) it has been identified that the load current waveform is unbalanced and nonsinusoidal. The developed method suppresses the distortions in the current waveform, with a view of reducing THD to 2.65% and load voltage to 0.37% which is much lesser than other techniques.. In addition, it regulates DLCV stable as highlighted in Fig 14(c) for fixed G and 25^0c of temperature.

At case 2, similar to case 1 the 30% of swell along with sag & the disturbance is inserted. Yet, proposed system identifies it successfully and suppresses it by introducing the required compensating voltage, as illustrated in Figure 15(a). The i_l waveform was found to be sinusoidal with unbalance in phases as given in Figure 15(b) due to unbalanced load 2. However, the developed technique reduces the THD of grid current to 3.83% and load voltage to 0.36%, which is lesser than other techniques. However, the developed method maintains constant DLCV, as Figure 15(c) shows.

Table 5 compares the THD of the proposed method with those of other standard techniques like PIC and SMC, and others exits in the literature survey. It exhibits that the projected system has lower THD while comparing with other techniques. However, Fig 16 represent the Current and Voltage FFT analysis of the current proposed system.

Table 5: THD comparison

	Method	THD					
		Source Current			**Load Voltage**		
		Phase-a	**Phase-b**	**Phase-c**	**Phase-a**	**Phase-b**	**Phase-c**
Case-1	**Proposed method**	**2.65**	**2.81**	**2.80**	**0.37**	**0.67**	**0.75**
	PIC	3.06	3.05	3.06	4.05	3.54	2.55
	SMC	2.84	2.84	2.82	4.07	4.39	4.01
	2L-UPQC [10]	5.42	5.43	5.61	4.03	3.86	4.04
	3L-UPQC [10]	4.72	4.45	4.86	3.37	3.27	3.36
	5L- UPQC [10]	3.85	4.09	4.40	3.02	2.97	3.03
	2L-UPQC-SRF [10]	5.47	6.07	5.95	4.45	4.76	4.99

_____

	3L-UPQC-SRF [10]	5.55	6.06	4.94	4.22	4.24	4.43
	5L-UPQC-SRF [10]	4.55	5.45	4.32	3.83	3.98	4.22
Case-2	**Proposed method**	**3.83**	**3.89**	**3.90**	**0.36**	**0.66**	**0.75**
	PIC	4.06	4.12	4.02	4.05	3.54	2.55
	SMC	3.98	3.98	3.99	2.89	4.12	3.47

(a) V_S, V_{se}, V_L

(b) I_S, I_{sh}, I_L

2945

_____
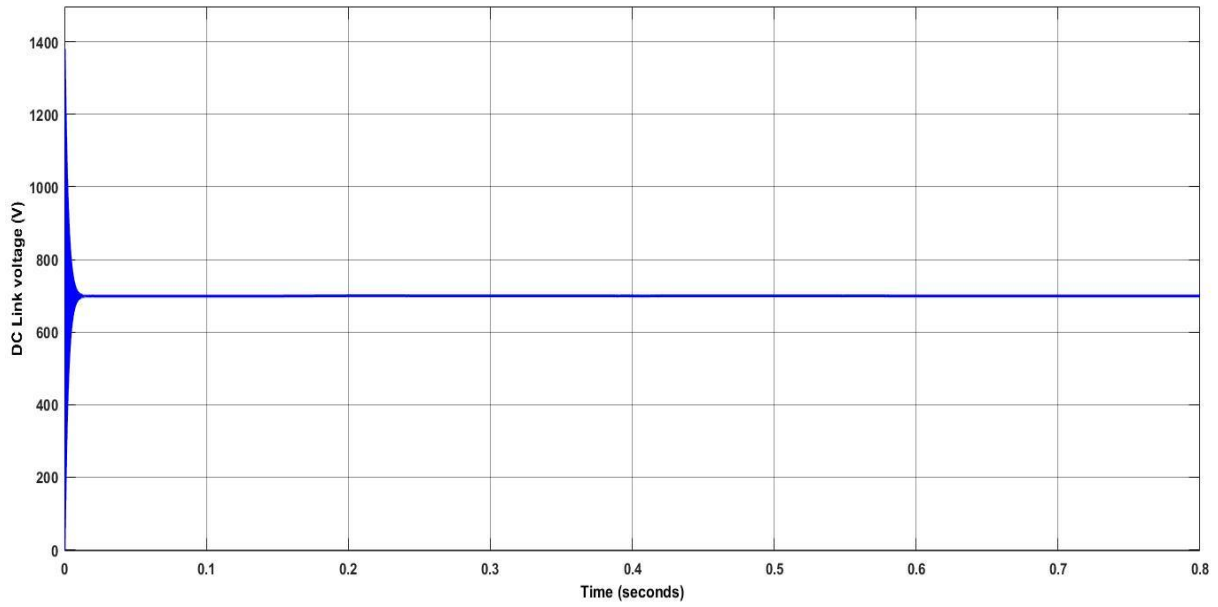
(c) DC Link Capacitor Voltage

Figure 14: Waveforms of the developed method for case1
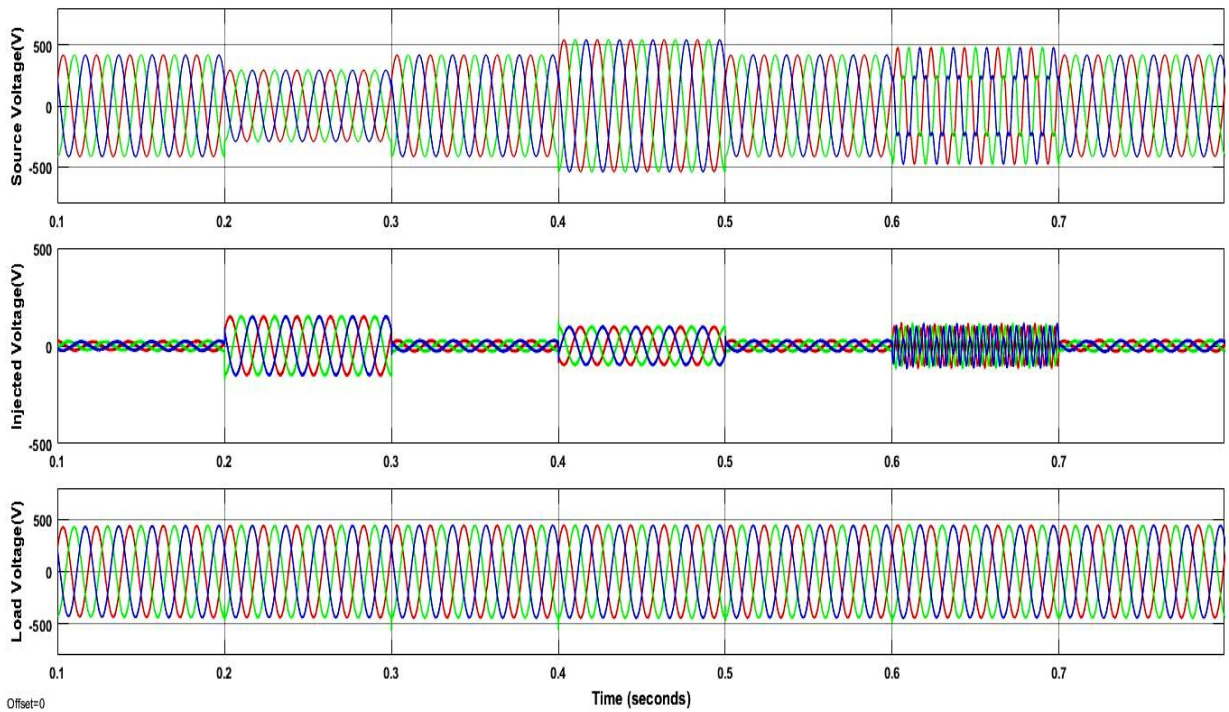
(a) V_S, V_{se}, V_L

_____
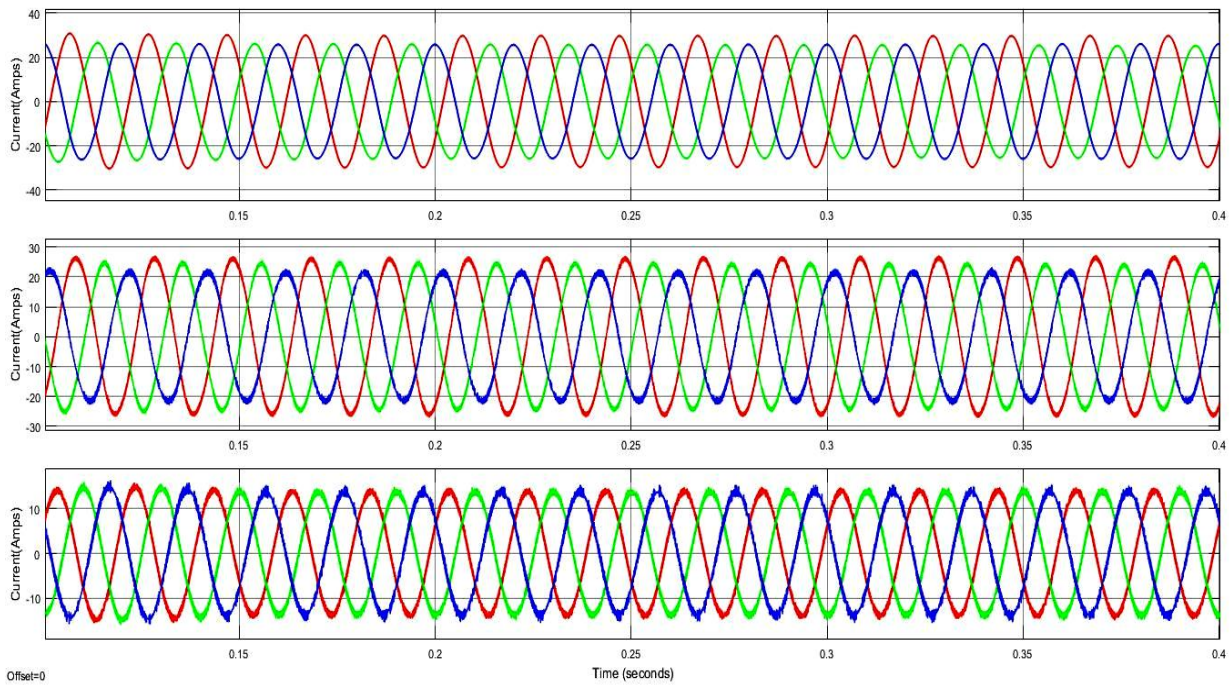
(b) I_S, I_{sh}, I_L
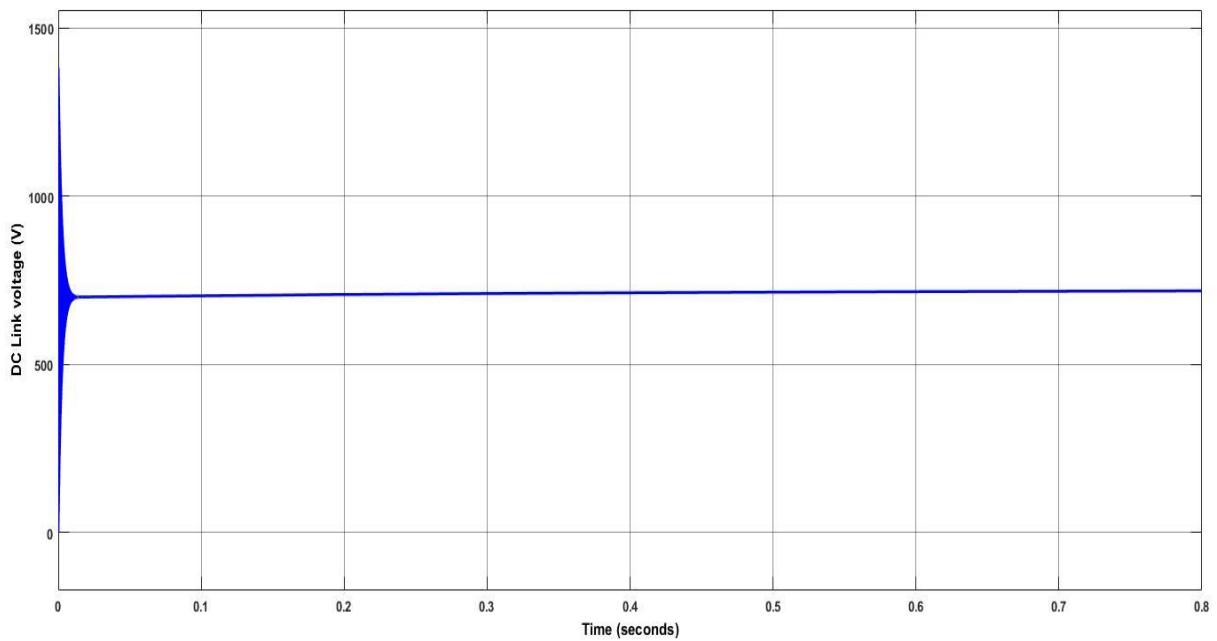
(C) DC Link Capacitor Voltage

Figure 15: Waveforms of the developed method for case 2.

_____
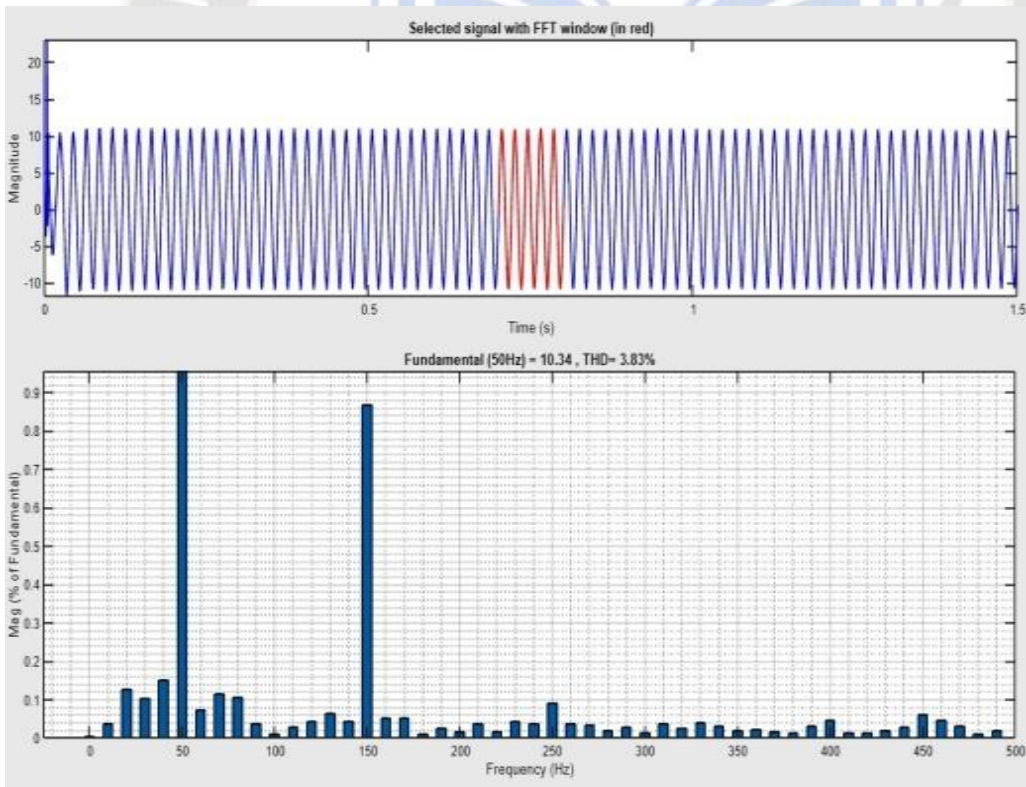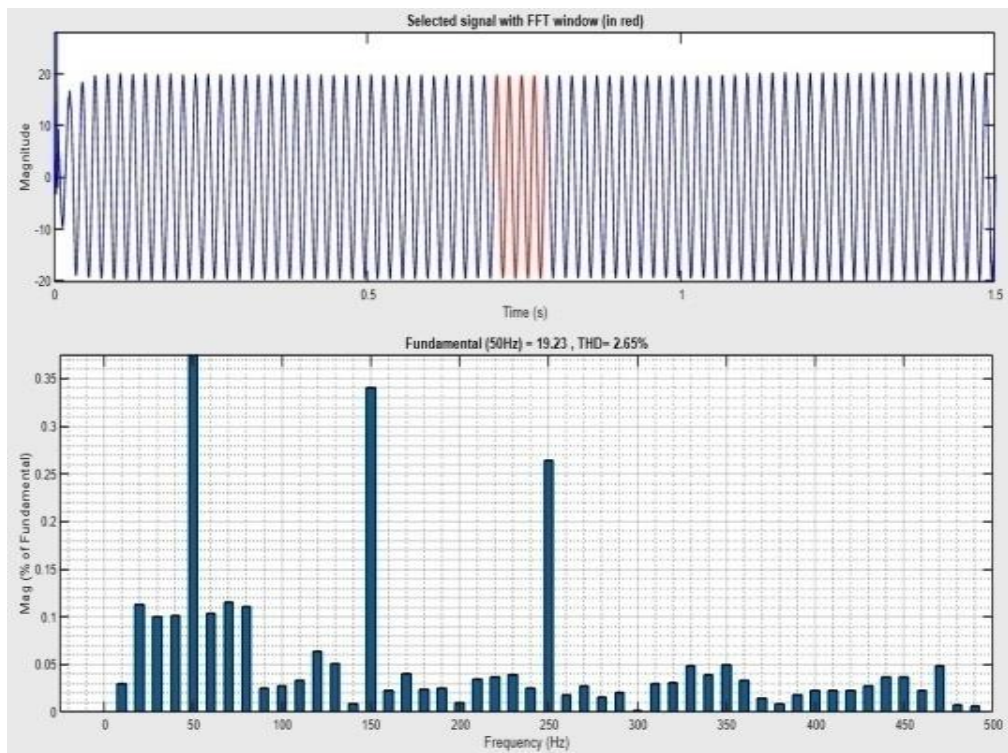
Case1

Case 2

Figure 16(a): Current THD spectrum for phase-a

_____
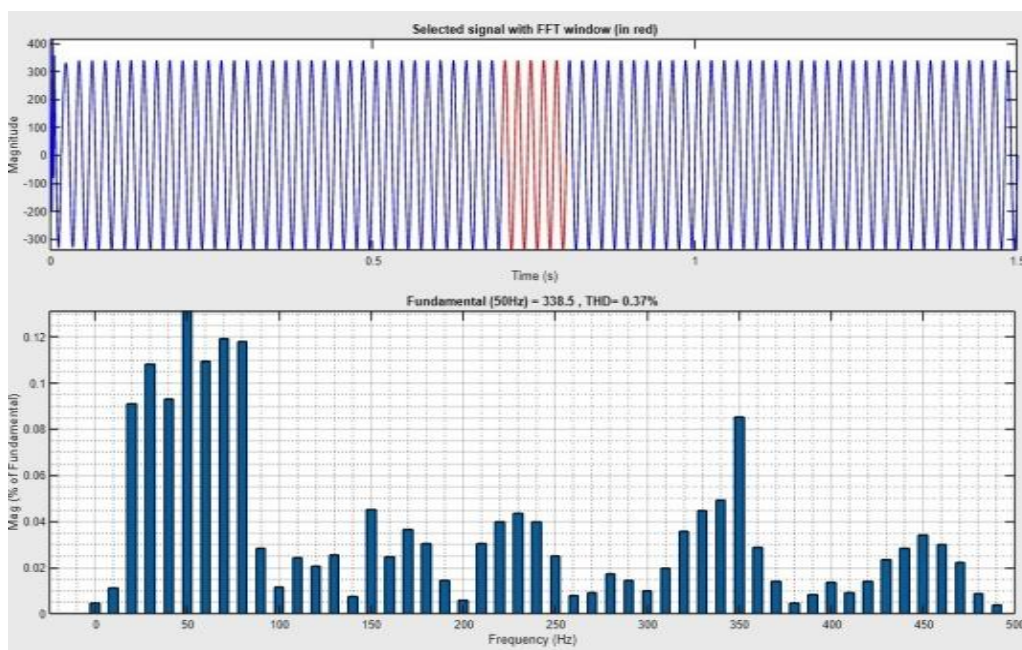
Case1
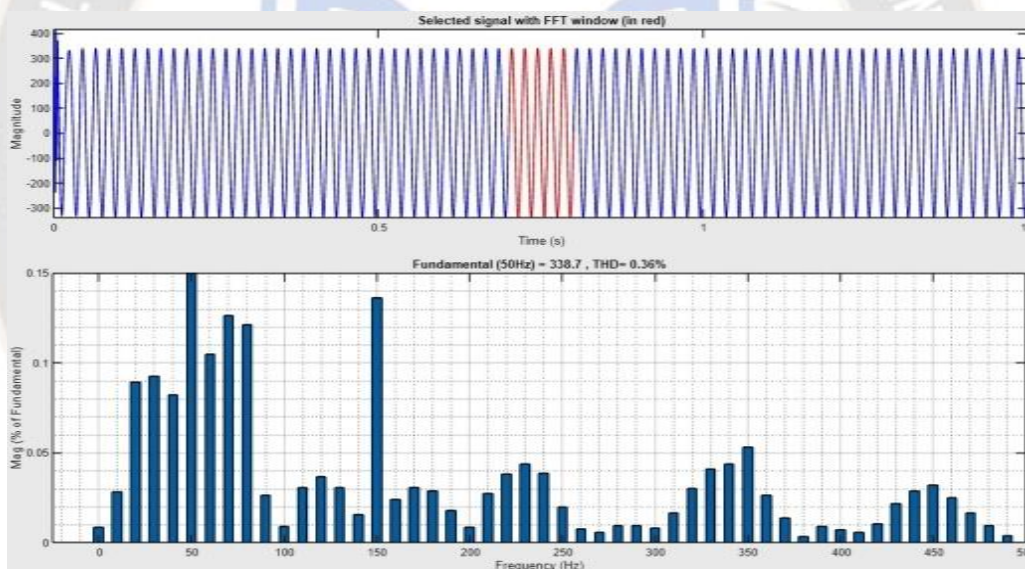
Case2

Figure 16(b): Voltage THD spectrum for phase-a

6. Conclusion

In this paper, a novel approach is introduced for a PV battery associated to a diode clamped five level UPQC utilizing an ANNC. In order to avoid the conventional abc-dq0-αβ conversions, the LMBP trained ANN controller is given to generate the necessary reference signals for shunt, series VSCs. However, the developed 5L-UPVBES maintains constant DLCV during loads variations, suppresses the current and voltage harmonics and improves the current and voltage waveform's shape, and eliminates the fluctuations of supply voltage (disturbance, sag and swell). To show the performance of the suggested system the comparison is done with PIC and SMC controllers for DLCV balancing and other methods available in literature. By, monitoring the results of the two cases it shows the developed system provides much lower THD compared with other techniques within the acceptable levels. The suggested method can be carried out using ANFIS control scheme in the future.

References

_____

1. Alok Kumar Mishra , Soumya Ranjan Das , Prakash K. Ray ,Ranjan Kumar Mallick, Asit Mohanty Dillip ,K. Mishra, PSO-GWO Optimized Fractional Order PID Based Hybrid Shunt Active Power Filter for Power Quality Improvements, IEEE Access, **DOI:** 10.1109/ACCESS.2020.2988611,Vol.8, pp. 74497 - 74512, May-2020

2. Koganti Srilakshmi, K. Krishna Jyothi, G. Kalyani & Y. Sai Prakash Goud. Design of UPQC with Solar PV and Battery Storage Systems for Power Quality Improvement. Cybernetics and Systems: An International Journal, March-(2023). DOI: 10.1080/01969722.2023.2175144.

3. Tzu-Chiao Lin , Bawoke Simachew, Intelligent Tuned Hybrid Power Filter with Fuzzy-PI Control, Energies 2022, 15, 4371. doi: 10.3390/en15124371.

4. Kumar Chandrasekaran, Jaisiva Selvaraj, Clement Raj Amaladoss, LogeshwariVeerapan, Hybrid renewable energy based smart grid system for reactive power management and voltage profile enhancement using artificial neural network, Energy Sources, Part A: Recovery, Utilization, and Environmental Effects, 2021, Vol. 43, No. 19, pp. 2419–2442, DOI: 10.1080/15567036.2021.1902430

5. Sayed, J.A.; Sabha, R.A.; Ranjan, K.J. Biogeography based optimization strategy for UPQC PI tuning on full order adaptive observer based control. IET Generation, Transmission & Distribution 2021, 15, 279-293.

6. Rajesh, P.; Shajin, F.H.; Uma sankar, L. A Novel Control Scheme for PV/WT/FC/Battery to Power Quality Enhancement in Micro Grid System: A Hybrid Technique. Energy Sources, Part A: Recovery, Utilization, and Environmental Effects 2021, 1-18.

7. Pazhanimuthu, C.; Ramesh, S. Grid integration of renewable energy sources (RES) for power quality improvement using adaptive fuzzy logic controller based series hybrid active power filter (SHAPF), Journal of Intelligent & Fuzzy Systems 2018, 35, 749–766.

8. Koganti Srilakshmi, Canavoy Narahari Sujatha, Praveen Kumar Balachandran, Lucian Mihet-Popa, and Naluguru Udaya Kumar, "Optimal Design of an Artificial Intelligence Controller for Solar-Battery Integrated UPQC in Three Phase Distribution Networks", Sustainability, Vol. 14, No. 21, Oct-2022.

9. Aruchamy Sakthivel, P. Vijaya kumar, A. Senthilkumar , L. Lakshminarasimman, S. Paramasivam: Experimental investigations on ant colony optimized pi control algorithm for shunt active power filter to improve power quality. Control Engineering Practice. (42), 153-169 (2015). https://doi.org/10.1016/j.conengprac.2015.04.013

10. SudheerVinnakoti, Venkata Reddy Kota, Implementation of artificial neural network based controller for a five-level converter based UPQC, Alexandria Engineering Journal, Elsevier, Vol 57, Issue 3, 2017, pp.1475-1488, https://doi.org/10.1016/j.aej.2017.03.027.

11. Alapati Ramadevi , Koganti Srilakshmi , Praveen Kumar Balachandran ,Ilhami Colak , C. Dhanamjayulu , and Baseem Khan. Optimal Design and Performance Investigation of Artificial Neural Network Controller for Solar- and Battery-Connected Unified Power Quality Conditioner. International Journal of Energy Research, Vol. 2023, 3355124, 22 pages, April-(2023).

12. Srilakshmi Koganti , Krishna Jyothi Koganti and Surender Reddy Salkuti , Design of Multi-Objective-Based Artificial Intelligence Controller for Wind/Battery-Connected Shunt Active Power Filter, Algorithms, Vol. 15, No. 8, pp. 256, 2022, DOI: 10.3390/a15080256.

13. Alapati Ramadevi , Koganti Srilakshmi , Praveen Kumar Balachandran ,Ilhami Colak , C. Dhanamjayulu , and Baseem Khan. Optimal Design and Performance Investigation of Artificial Neural Network Controller for Solar- and Battery-Connected Unified Power Quality Conditioner. International Journal of Energy Research, Vol. 2023, 3355124, 22 pages, April-(2023).

14. Koganti Srilakshmi ,Nakka Srinivas , Praveen Kumar Balachandran , Jonnala Ganesh Prasad Reddy, Sravanthy Gaddameedhi, NagarajuValluri, ShitharthSelvarajan, Design of Soccer League Optimization Based Hybrid Controller for Solar-Battery Integrated UPQC, IEEE Access, Vol. 10, pp. 107116-107136, 2022, DOI: 10.1109/ACCESS.2022.3211504.